Egyptian Geophysical Society
EGS Journal, vol. 5, No. 1, 33-49 (2007)

DEVELOPMENT DIRECTIONS OF THE PALEOZOIC RESERVOIRS IN OCTOBER OIL FIELD BASED ON PETROPHYSICAL PROPERTIES

M.M. Gadallah[1], R.A. El-Terb[2], E.M. El Katan[2] and I.M. El Alfy[2]

[1] *Geology Department, Faculty of Science, Zagazig University.*
[2]*Exploration Division, Nuclear Materials Authority.*

تنمية خزان الباليوزوى فى حقل بترول أكتوبر اعتماداً على الخواص البتروفيزيائية للصخور

الخلاصة: تم استخدام تحاليل العينات اللبية لعدد ٤٩٤ عينة وأيضا تحليل تسجيلات الآبار لعدد ٨ آبار وذلك لاستنتاج الخواص البتروفيزيائية وتقييم خزان الباليوزوى فى حقل بترول أكتوبر بخليج السويس. تعكس التحاليل الإحصائية لقيم المسامية والنفاذية زيادة السعة التخزينية لهذه الصخور مع عدم تجانسها. تم استنتاج معاملات الخزان المختلفة مثل معامل التماسك والتشبع من تحاليل العينات اللبية الخاصة والتى تستخدم فى تحاليل تسجيلات الآبار. ويبدأ تحليل تسجيلات الآبار فى خزان الباليوزوى بترقيم البيانات أى تحويل البيانات من صورة منحنيات إلى أرقام لسهولة التعامل معها. ثم عمل قاعدة بيانات وعمل تصحيحات بيئية لهذه الآبار وذلك لتقليل احتمالية حدوث أخطاء فى تحليل هذه الآبار.

تم توضيح نتائج تحاليل الآبار راسياً عن طريق رسم قيم التشبع الليثولوجى وأفقياً عن طريق رسم الخرائط للمعاملات المختلفة.

وقد أمكن استنتاج النفاذية من تسجيلات الآبار وتحاليل العينات وعمل علاقات لاستنتاج قيم النفاذية فى الآبار التى لم يتم قياس عينات لبية لها وكانت طريقة الشبكة العصبية الاصطناعية هى أفضل الطرق لاستنتاج النفاذية من تسجيلات الآبار. كما تم عمل خريطة لتحديد أفضل الأماكن لتطوير تنمية هذا الخزان باستخدام برامج حاسوبية متطورة معتمدة على عدد ١٢ معامل مختلف لصخور الخزان الباليوزوى.

ABSTRACT: *Core analysis results of 494 core samples and log analysis in eight wells are used to evaluate the petrophysical properties of the Paleozoic reservoirs in October Oil Field. Statistical analysis and cumulative frequency of porosity and permeability reflected the high storage capacity and heterogeneity of Paleozoic reservoirs. Special core analysis of the Paleozoic reservoirs identified the cementation factor and saturation exponent which are used in well log analysis.*
Well log analysis of the Paleozoic reservoirs in the study wells passed through, digitizing of well logs using scanner and Grapher program, editing data base and environmental corrections for the studied logs, then normalizing the logs in order to reduce the probability of major errors and inconsistencies in log analysis results. The results of log analysis are illustrated vertically by lithosaturation analog and laterally by reservoir isoparametric maps. The findings are useful to isolate zones for possible testing and indicated the northwest and south directions as candidates for future field development.

INTRODUCTION

The study area is located at the middle part of the Gulf of Suez and it located between longitudes 33° 10` and 33° 25` E and latitudes 28° 45` and 29° 10` N (Fig. 1). The Nubia sandstone represents the main producing horizon in October Oil Field. The Nubia sandstone overlies the basement rocks and underlies the Pre-Cenomanian rocks. It is subdivided in the subsurface into four informal lithologic units arranged from top to bottom; Nubia A, Nubia B, Nubia C and Nubia D (Fig. 2).

In the present study, the measurements of porosity and permeability of 493 core samples and measurements of water saturation, formation factor and the resistively index of 45 core samples and well logging data of eight wells are used to evaluate the petrophysical characteristics of the Paleozoic deposits and development the study Field.

There are many methods are used to estimate the permeability such as conventional method and optimal method. The artificial neural network is the best method to estimate the permeability from well logging data and the core samples.

Multi-well normalization method is very important technique in the well logging study because, more than fifty percent of well log data need to be corrected for bore hole conditions, calibration errors or shift depths (Neinast and Knox, 1974).

The results of well logs analysis of October wells are illustrated vertically by litho-saturation cross-plots and laterally by isoparametric maps. There are twelve parameters can be estimated from the well logs analysis and it can be used there parameters together to make the development map by using the GIS software.

METHODOLOGY

The core analysis reports explain that, the samples were cut every foot with one inch diameter for petrophysical measurements. These plug were cleaned using solvent extracted in refluxing methanol and zylene to remove the traces of brine and oil from the Paleozoic samples. These core samples were dried in conventional and special laboratory ovens. Fluid summation porosity, Helium porosity, horizontal and vertical permeabilities, water saturation, resistivity index and formation factor were measurements. The available well logging data in the studt field are digitized using scanner and grapher 2.03 program. After digitizing all logs, the data processing of well logs is performed on all well logs. It includes data base editing and data correction. Data base editing means confirming the digitized well log data with original curves to be identical. Flagging the missing and bad data and reconstruct it. Environmental corrections were applied for the gamma ray, density, neutron and resistivity logs in the studied wells. Data correction means normalizing the well log data to ensure that, it is accurate, consistent and correlated well to well. The corrected data of well logs were used to evaluate the reservoir parameters of Paleozoic sediments using LOGANAL software. The reservoir parameters include gross thickness, net pay thickness, total porosity, effective porosity, shale volume, water saturation, bulk pore volume and oil in place indicator. The bulk pore volume (PHIH) can be calculated using the equation PHIH = (PHI* integrated net pay) while the oil in place indicator (HPVH) is calculated using this equation HPVH = (integrated PHIH * (1-Sw)).

On the other hand, the net pay thickness is calculated using 10% or more for effective porosity, 35% for shale volume and 50% or less for water saturation. The common approach is to develop a core permeability versus log porosity relationship by regression and then, to predict permeability in uncored wells from logs. The general expression proposed by Wyllie and Spangler (1952) is:

$$K = \frac{\phi}{kS_p^2}$$

K = permeability Φ = porosity

k = Kozeny constant S_p = Surface area / unit volume of pore space

The optimal transformation method for permeability estimation involves the transformation of Petrophysical data to obtain the maximum correlation between observed variables. It is a general and computationally efficient non-parametric algorithm called the alternating conditional expectation (ACE) which was originally proposed by Breiman and Friedman (1985). The algorithm provides a method for estimating transformations of raw log data in multiple regressions without prior assumptions of a functional relationship to estimation permeability.

The artificial neural network is stated by Thompson et al. (1996). It is a new data processing mechanism that allows an easy transformation of well logging data of the Paleozoic sediments in October oil field to permeability estimation. Neural network is a set of highly connected nodes or processing elements, modeled loosely after biological neurons. ANN is trained by giving them example problems and having them produce a solution. This is repeated thousands of times, until the rate of correct solutions produced reaches acceptable levels. It is critical that the ANN learns from good data. The fundamental design of a black-propagation neural network consists of an input layer, hidden layers, and an output layer. The goal of training is to reach an optimal solution based on the performance measurements to evaluate the practical application of ANN. The predicted neural permeability should be compared with core permeability. If the neural permeability matches the core permeability, the investigator can be reasonably confident that, the ANN can be applied for estimating permeability in uncored intervals and wells.

The GIS software can be used in statistical analysis and mapping, we are used this software to development the October oil field by drawing the development or decision map which depended on the all parameters we can get them from the analysis of well logging data.

RESEERVOIR EVALUATION:

CORE ANALYSIS

a. Conventional Core Analysis

Figure (3) illustrate the histogram frequency and cumulative frequency for porosity and permeability, from this figure the porosity varies from 1% to 34.7% and the main porosity for the Nubia samples is 14.88%. The permeability for the same samples varies from 0.01 md to 9327 md, while the main value of permeability is 262.1 md.

The relationship between fluid summation and helium porosity in GS 195-2b well is represented by positive trend. It means that, fluid summation porosity increases with the increasing of helium porosity. This relationship is represented in figure (4). The correlation coefficient of this relation is 0.66 and the linear regression equation for this relation is represented as:

$$\Phi_h = 0.6646\ \Phi_s + 3.1154$$

From this equation, the helium porosity gives high values than the fluid summation porosity in the range less than 10% porosity due to the micro pores, but the fluid summation porosity is higher than the helium porosity in the range more than 10% porosity due to the macro pores and the clay minerals.

The relationship between the vertical and horizontal permeabilities in GS 195-2b well is shown in figure (5). This relationship has a positive trend and the correlation coefficient of this relation is 0.93 and the linear regression equation is:

$$K_v = 0.6367 K_h^{0.94}$$

The relationships between porosity and permeability for wells GS 195-2b and GS 196-2a are shown in figure (6). In well GS 195-2b the correlation coefficients for fluid summation porosity and horizontal and vertical permeabilities are 0.59 and 0.55 respectively. The linear regression equations are:

$$K_h = 0.0505 e^{0.284\,\phi_s} \quad \text{and} \quad K_v = 0.0381 e^{0.2676\phi_s}$$

The correlation coefficients for helium porosity and horizontal and vertical permeabilities are 0.66 and 0.62 respectively. The linear regression equations are:

$$K_h = 0.0516 e^{0.323\,\phi_h} \quad \text{and} \quad K_v = 0.0382 e^{0.306\,\phi_h}$$

In case of well GS 196-2a the relationship is represented between helium porosity and horizontal permeability, the correlation coefficient for this relation have positive value and it is equal 0.82 and the linear regression equation is:

$$K_h = 0.0692 e^{0.4312\phi_h}.$$

b. Special Core Analysis

The relationship between porosity and formation resistivity factor of Paleozoic samples in well GS 195-2b is shown in Figure (7a). The cementation factor equals to 2.363, while the correlation coefficient equals – 0.91. The linear regression equation representing the strong negative trend is

$$F = 0.882 * \Phi^{-2.363}$$

The plot of the formation factor and permeability of the studied core samples of well GS 195-2b is shown in Fig. (7b). From the plot we can say that, the correlation coefficient of this relation has equals to – 0.5. The linear regression equation controls this relationship is:

$$F = 24.98\ K^{-1.059}$$

The relationship between (I) and (S_w) of well GS 195-2b is shown in Figure (7c). From this relation the saturation exponent (n) is equal to 2.02, and the correlation coefficient of this relation has a very strong negative trend where it is equal to – 0.995, the linear regression equation can be discussed as:

$$RI = 1.0506\ S_w^{-2.02}$$

The relationship between resistivity index and permeability of well GS 195-2b is shown in Figure (7d). It represents by strong positive trend with correlation coefficient equals to 0.93. The linear regression equation is

$$RI = 0.0347\ K^{0.9065}$$

The relationship between S_w and K at well GS 195-2b is shown in Figure (7e). It represents by strong negative trend with correlation coefficient equals to – 0.93. The linear regression equation we can obtain to the water saturation from permeability is: $S_w = 604.98\ K^{-0.49}$

Permeability Estimation from Well Logs:

Figure (8a) represents the relationships between log porosity and either core porosity or core permeability in well GS 195-2 from October Oil Field. These relationships represent by positive trends with correlation coefficient 0.52. The linear regression equation is represented on the figure.

The relationships between core porosity and optimal porosity and between core permeability and optimal permeability of Paleozoic sediments in October Oil field, is represented in figure (8b). The correlation coefficient of this relation is about 0.75 and the linear regression equation is shown in the figure. The optimal transformation model of Paleozoic sediments in the study Field can be used to estimate permeability profiles in the remainder of the reservoir and close offset wells that were drilled without coring. The correlation coefficient is much higher than that obtained by traditional correlation of core permeability with porosity.

The predicted permeability and porosity from neural network was correlated with the core permeability and porosity from the logs of the studied wells as illustrated in figure (8c). The correlation coefficients of these relations are 0.92 for training and 0.95 for test as in figure (8d).

From these perfect relations, the porosity and permeability could be estimated for an independent well without core measurements information for Paleozoic sediments.

LITHOSATURATION:

a. Total distribution of Lithosaturation values.

Figure. (13a) shows that the total lithologies and fluids distributions of well GS 160-2. It consists mainly of sandstone which reaches about 45 % from the total lithology percent. The volume of shale percent is 15.2 %, while the percents of limestone and dolostone are 13.08 % and 7.51 % respectively. The effective porosity of this well is 19.92 % and it occupies by 6.26 % water, 3.34 % residual hydrocarbons and 10.32 % movable hydrocarbons.

Table (1): Shifts values for normalizing the data in the study wells.				
Well name	**Gamma ray, (API)**	**Bulk density, (gm/cc)**	**Neutron porosity, (%)**	**Sonic log (transit time), (µs/ft)**
GS 160-2	-3	0.01	1	-1
GS 173-2	-5	-0.01	1	-
GS 195-2	1	-0.01	-1	-
GS 196-1	-1	-0.01	-1	-
GS 196-2	-2	0.01	-1	-
GS 197-1	-1	0.01	1	-
GS 206-1	-4	0.01	1	-
GS 207-1	4	0.01	-1	1

The total lithology distribution of well GS 173-2 (Fig. 13b) consists mainly of 55.37 % sandstone from the total lithology.

The relatively fair correlation coefficients of either traditional or optimal transformation methods reflect high variability of permeability. To estimate permeability from log data it is better to use the neural network than both traditional logarithmic and optimal transformation because of the relatively high correlation coefficient.

WELL LOG ANALYSIS

Multi-well Normalization.

The required shift to ensure a good matching between the individual gamma ray histogram of well GS 160-2 and the standard histogram is -3 API as it shown in figure (9). A shift of 0.01 gm/cc as in figure (10) was required to ensure a good matching between the individual density histogram of well GS 160-2 and the standard histogram. Figure (11) illustrate that, the shift of 1% was required to ensure a good matching between the individual neutron histogram of well GS 160-2 and the standard histogram. Also the shift of -1 µs/ft was required to ensure a good matching between the individual sonic histogram of well GS 160-2 and the standard histogram as in figure (12). The table (1) illustrate the shifts were required for the all logs in October oil field:

The volume of shale percent is 5.22 %, and the percents of limestone and dolostone are 10.81 % and 12.65 % respectively. The effective porosity of this well represented by 15.98 % from the total volume of the rock and it occupies by 10.07 % water, 0.72 % residual hydrocarbons and 5.19 % movable hydrocarbons.

Figure. (13c) shows the total lithology and fluid distribution of well GS 195-2. It consists mainly of sandstone which reaches about 54.46 % from the total lithology. The volume of shale percent is 20.03 %, while the percents of limestone and dolostone are 9.05 % and 2.09 % respectively. The effective porosity of this well is 14.37 % and it occupies by 6.94 % for water, 2.69 % for residual hydrocarbons and 4.74 % for movable hydrocarbons.

The total lithology distribution of well GS 196-1 (Fig. 13d) consists mainly of 49.5 % sandstone, 26.27 % shale, 9.27 % limestone and 3.64 % dolostone. The effective porosity is 12.77 % and it occupies by 10.92 % water, 0.39 % residual hydrocarbons and 1.46 % movable hydrocarbons.

Figure (13e) shows the total lithology and fluid distributions of well GS 196-2. It consists mainly of sandstone (51.15 %), shale (5.06 %), limestone (18.89 %) and dolostone (9.19 %), respectively. The effective porosity of this well is 17.29 % and it occupies by 12.4 % water, 1.08 % residual hydrocarbons and 3.81 % movable hydrocarbons.

The total lithology and fluid distribution of well GS 197-1 (Fig. 13f) consists mainly of sandstone with 63.2 %, shale with 6.94 %, limestone with 8.83 % and dolostone with 4.82 % respectively. The effective porosity of this well is 16.02 % and it occupies by 10.36 % water, 1.80 % residual hydrocarbons and 3.86 % movable hydrocarbons.

Figure (13g) shows the total lithology distribution of well GS 206-1. It consists mainly of sandstone, shale, limestone and dolostone with percentage values of 45.67 %, 25.63 %, 9.93 % and 11.62 % respectively. The effective porosity of this well is 8.13 % and it occupies by 4.29 % water, 2.1 % residual hydrocarbons and 1.74 % movable hydrocarbons.

The total lithology distribution of well GS 207-1 (Fig. 13h) consists mainly of sandstone with 41.93 %, shale with 2.9 %, limestone with 12.48 % and dolomite with 5.03 % respectively. The effective porosity of this well is 35.04 % and it occupies by 6.76 % for water, 12.03 % for residual hydrocarbons and 16.25 % for movable hydrocarbons.

Figure (13i) shows the total lithology and fluid distributions of the total area under study. It consists mainly of sandstone 50.8 %, shale 13.4 %, limestone 11.5 % and dolomite 7.1 % respectively. The effective porosity of this well is 17.42 % and it occupies by 8.5 %

for water, 3 % for residual hydrocarbons and 5.92 % for movable hydrocarbons.

b. Vertical distribution of Petrophysical and lithology results

1) Lithosaturation analog of well GS 160-2

The lithosaturation crossplot of Paleozoic Nubia in well GS 160-2 (Fig. 14a) shows that, this section can be classified into three distinguished intervals. The first interval ranges from depth 11107 ft. to depth 11750 ft. it reflects that the predominance lithology is sandstone which reaches to 60% with some intercalations of shale and limestone. It has good effective porosity with appreciable hydrocarbons in the places of high porosity intervals.

The second interval ranges from depth 11750 ft. to depth 12210 ft. It illustrates the predominance of shale with sometimes negligible porosity. There are many intercalations of sandstone and streaks of carbonate in this interval. The hydrocarbon saturations in this interval are generally small to moderate percent.

The third interval ranges from depth 12210 ft. to depth 12602 ft. It consists mainly of carbonatic limestone, sandstone with little intercalations of shale. The hydrocarbon fluids in this interval are small.

2) Lithosaturation analog of well GS 173-2

Figure. (14b) represents the lithosaturation crossplot of the Paleozoic Nubia in well GS 173-2. It is classified into two intervals. The first interval starting from depth 13421 ft. to depth 13640 ft. It reflects that the main component rock in this interval is the dolostone, sandstone and small amount of shale volume. The water saturation of this interval reaches 65% while the hydrocarbon saturation has a small value.

The second interval starts from depth 13640 ft. to depth 13849 ft. It consists mainly of sandstone, little intercalations of limestone and dolostone with little bit amount of shale. The fluids in this interval is mainly water with rare values of movable hydrocarbons.

3) Lithosaturation of well GS 195-2

The lithosaturation analog of Paleozoic Nubia in well GS 195-2 (Fig. 14c) shows that this section can be classified into three intervals. The first interval starts from depth 11164 ft. to depth 11450 ft. It consists mainly of shaly sandstone with some intercalations of limestone streaks. According to the high values of shale contents in this interval, the effective porosity represents by small to moderate values. The water saturation fluid in this interval is moderately amount with small amount of hydrocarbon.

The second interval ranges from depth 11450 ft. to depth 11770 ft. It consists mainly of sandstone rock with little intercalation of limestone and dolostone streaks. The volume of shale in this interval is very small thus the effective porosity is good. The water saturation percent is moderate while the hydrocarbon saturation percent is high.

The third interval ranges from depth 11770 ft. to depth 11964 ft. It reflects that the predominance lithology is shale with some intercalation of sandstone and limestone. According to the high value of shale in this interval, the effective porosity is poor and the water and hydrocarbon saturations have a small amount.

4) Lithosaturation of well GS 196-1

Figure. (14d) illustrates the lithosaturation analog of Paleozoic Nubia in well GS 196-1. This section can be classified into three distinguished intervals. The first interval starts from depth 12177 ft. to depth 12255 ft. It consists mainly of shaly sandstone with some intercalations of limestone. According to the high values of shale contents in this interval, the effective porosity represents by poor to fair. The water saturation of this interval is generally high amount with small amount of the hydrocarbon saturation.

The second interval ranges from depth 12255 ft. to depth 12470 ft. It consist mainly of sandstone rock with little intercalation of limestone and dolomite streaks. the volume of shale is small thus the porosity in this interval is good. The water saturation percent is high, while the hydrocarbon saturation percent is small.

The third interval starts from depth 12470 ft. to depth 12538 ft. It reflects that, the predominance lithology is shale with some intercalation of sandstone and limestone. According to the high value of shale, the effective porosity is negligible with little amount of water and hydrocarbons.

5) Lithosaturation of well GS 196-2

The Lithosaturation crossplot of Paleozoic Nubia of well GS 196-2 is shown in Figure. (15a). It can be classified into four distinguished intervals. The first interval starts from depth 11550 ft. to depth 11660 ft. It consists mainly of carbonates with some intercalations of sandstone. The shale percent is very small which reflects fair to good effective porosity. The water and the hydrocarbon saturation reflect moderate amount of fluids.

The second interval ranges from depth 11660 ft. to depth 11790 ft. It consists mainly of sandstone rock with intercalation of dolomite, The volume of shale is very small thus the effective porosity is good. The water and hydrocarbon saturations are found with moderate amount.

Well Name	**Growth thickness ft**	**Net-pay (ft)**	**Phit (%)**	**Phie (%)**	SW **(%)**	VSH **(%)**	SXO **(%)**	SH **(%)**	SHR **(%)**	SHM **(%)**	BPV **(ft)**	OIP **(ft)**
GS 160-2	1496	1211	23.7	19.8	38.1	15.1	84.6	61.9	15.3	46.5	240	148
GS 173-2	428	109	19.2	17.8	65.4	5.22	96.2	34.5	3.77	30.7	19.4	6.7
GS 195-2	806	373	19.4	14.4	54.5	22.1	83.6	45.4	16.3	29.1	54.0	24.5
GS 196-1	361	12	17.8	12.7	86.4	28.7	97.4	13.5	2.54	11.0	1.53	0.27
GS 196-2	459	114	18.5	18.5	72.5	5.06	94.5	27.4	5.49	22.0	21.1	5.81
GS 197-2	329	82	17.6	16.2	70.1	6.94	90.8	29.8	9.11	20.7	13.3	3.97
GS 206-1	153	8	9.88	7.09	70.2	27.7	91.6	29.7	8.32	21.4	0.56	0.17
GS 207-1	206	203	31.1	30.8	20.3	3.91	66.4	79.8	33.5	46.1	62.6	49.9

The third interval ranges from depth 11790 ft. to depth 11920 ft. It reflects that the predominant lithology is limestone and dolomite with some intercalations of sandstone. According to the low value of shale in this interval so the effective porosity is good, and so, there is a big amount of water with little hydrocarbon saturations.

The fourth interval starts at depth 11920 ft. and ends at depth 12005 ft. It indicates that, the predominant lithology is sandstone with little intercalations of limestone and shale. The water saturation in this interval is high with little amount of hydrocarbon saturations.

6) Lithosaturation of well GS 197-1

The lithosaturation analog of Paleozoic Nubia in well GS 197-1 (Fig. 15b) shows that this section can be classified into three distinguished intervals. The first interval ranges from depth 13104 ft. to depth 13175 ft. this interval consists of mainly carbonitic limestone and dolomite with some intercalations of sandstone. The shale percent is moderate thus the porosity value generally moderate to high. The water saturation fluid in this interval is generally moderate amount and also the hydrocarbon fluid is generally moderate amount.

The second interval ranges from depth 13175 ft. to depth 13390 ft and it consist mainly of sandstone rock with little intercalation of limestone. The volume of shale is very small thus the porosity in this interval is high. The water saturation percent is high and the hydrocarbon has a small to moderate percent.

The third interval ranges from depth 13390 ft. to depth 13437 ft. It reflects that the predominance of carbonitic limestone and dolomite with intercalation from sandstone. The shale percentage ranges from small to moderate so the porosity is moderate to high, and so it is moderate amount of water saturation and also of hydrocarbons.

7) Lithosaturation of well GS 206-1

Figure (15c) represents the lithosaturation crossplot of the Paleozoic Nubia in well GS 173-2. It is classified this section into two intervals. The first interval ranges from depth 12581 ft. to depth 12712 ft. This interval consists mainly of shaly sandstone with intercalations of carbonitic limestone and dolomite. According to the high value of the shale content of the porosity value is generally low. The water saturation and the hydrocarbons have little amount in this interval.

The second interval starts from depth 12712 ft. to depth 12734 ft. and it consist mainly of shale and carbonatic limestone and dolomite with intercalation of the sandstone. According to the high value of shale volume thus the porosity in this interval is low. The water saturation and the hydrocarbons have little amount in this interval.

8) Lithosaturation of well GS 207-1

The lithosaturation analog of Paleozoic Nubia in well GS 207-1 (Fig. 15d) shows that, this section reflects one distinguished interval. The lithology of this well consists mainly of sandstone with some limestone and dolomite streaks. The shale content is very low. It has high values of effective porosity with small to moderate amount of water saturation and moderate to high amount of hydrocarbon saturations.

RESERVOIR MAPPING

The results of well log analysis for the Paleozoic Nubia Formations of October wells are listed in table (2).

These parameters are contoured to show the lateral distribution of these Petrophysical parameters.

The total thickness map of Paleozoic Nubia Formations (Fig. 16a) shows that the thickness increases toward the northwest, while it decreases toward southeast. The Paleozoic Nubia Formations have the maximum thickness, 1496 ft, at well GS 160-2 and the minimum thickness, 153 ft, at well GS 206-1.

The net-pay thickness distribution map (Fig. 16b) demonstrates that the net-pay thickness increases toward the northwest and decrease gradually toward the southeast. The maximum net-pay thickness is shown at well GS 160-2, it is 1211 ft. The minimum net-pay thickness is 8 ft. which is recorded at well GS 206-1.

The total porosity distribution map (Fig. 16c) shows that the total porosity increases toward the northwest and south while the total porosity decreases gradually toward the southeast. The maximum value of total porosity is recorded at well GS 207-1 and it is 31.1 %. While the minimum value of total porosity is recorded at well GS 206-1 and it is 9.88 %.

Figure (16d) represents the effective porosity distribution map for Paleozoic Formations which increases toward the northwest and the south to reach 30.86 % at well GS 207-1. While the effective porosity decreases gradually toward the southeast and the center of the area to reach 12.77 % at well GS 196-1 and it increases to reach 18.54 % at GS 196-2 well and it decreases gradually toward the southeast to record the minimum value, 7.09 % at well GS 206-1.

The shale content distribution map (Fig. 16e) indicates that the maximum value of shale content is recorded at the center of the area (28.79 %). It is recorded at well GS 196-1. The shale content values are decreased toward the northwest direction after that it increases in the same direction to reach 15.15 % at well GS 160-2. Also the shale content increases from the center toward southeast to reach 27.75 % at well GS 206-1. After that, it decreases towards the south to record 3.91 % at well GS 207-1.

Figure (16f) shows the distribution of the water saturation in the flushed zone. We note that the maximum value is recorded at the center of the area. The maximum value 97.46 % is recorded at well GS 196-1. From the figure we can note that the water saturation in the flushed zone decreases towards the northwest and the south directions and the minimum value 66.43 % is recorded at well GS 207-1.

The water saturation distribution map (Fig. 16g) indicates that the maximum value 86.46 % of water saturation is recorded at the center of the area at well GS 196-1, and the water saturation in the area decreases gradually toward the northwest and toward the south to reach the minimum value 20.32 % at well GS 207-1 on the south of the area.

The hydrocarbon saturation distribution map (Fig. 16h) shows that the minimum hydrocarbon saturation value 13.54 % is recorded at the center of the area at well GS 196-1. The values of the hydrocarbon saturation in the area increase gradually from the center toward the northwest direction recording 61.9 % at well GS 160-2. The value is increased gradually toward the south direction recording 79.68 % at well GS 207-1.

The residual hydrocarbon saturation distribution map (Fig. 17a) indicates that the minimum value of the residual hydrocarbon saturation is 2.54 % which recorded at well GS 196-1 at the center of the area. The values of residual hydrocarbon saturation are increased gradually toward northwest direction to reach 15.39 % at well GS 160-2. It is increased gradually toward the south direction to reach the maximum residual hydrocarbon saturation value 33.57 % at well GS 207-1.

Figure (17b) shows that the distribution of the movable hydrocarbon saturation of the Paleozoic rocks in October oil field. It indicates that the minimum value 11 % is recording at the center of the area at well GS 196-1. Also from this figure we can notes that the movable hydrocarbon saturation values are increased gradually from the center toward the northwest and the south directions. The maximum value 46.52 % of the movable hydrocarbon saturation was recorded at well GS 160-2.

The bulk pore volume distribution map (Fig. 17c) indicates that, the maximum value 240 ft. of the bulk pore volume in the area is recorded at well GS 160-2. The values of bulk pore volume are decreased gradually toward the center of the area and it is increased from the center toward the south to reach 0.567 ft at GS 206-1 well, and it is increased at well GS 207-1 in the south to record 62.65 ft.

The oil in place distribution map (Fig. 17d) indicates that the maximum value of the oil in place in the study area is recorded at the northwest side of the area at well GS 160-2 recording 148.65 ft, while the minimum value of the oil in place in the study area is recorded at the southern side of the area at well GS 206-1 recording 0.17 ft. The oil in place values were decreased gradually from the northwest and the south directions toward the center of the area.

DEVELOPMENT or DESCISION MAP

Twelve Parameters were estimated from the well log date by the LOGANAL software are used to estimate the development map by using the GIS software. The development map depended on the all parameters thus it is better than the maps which depend on one parameter. The GIS software can be used to produce two development maps. Figure (18 a & b) illustrate the development maps which illustrates that, it can be development the wells in October oil Field in the South and North West directions as it estimated before by the maps.

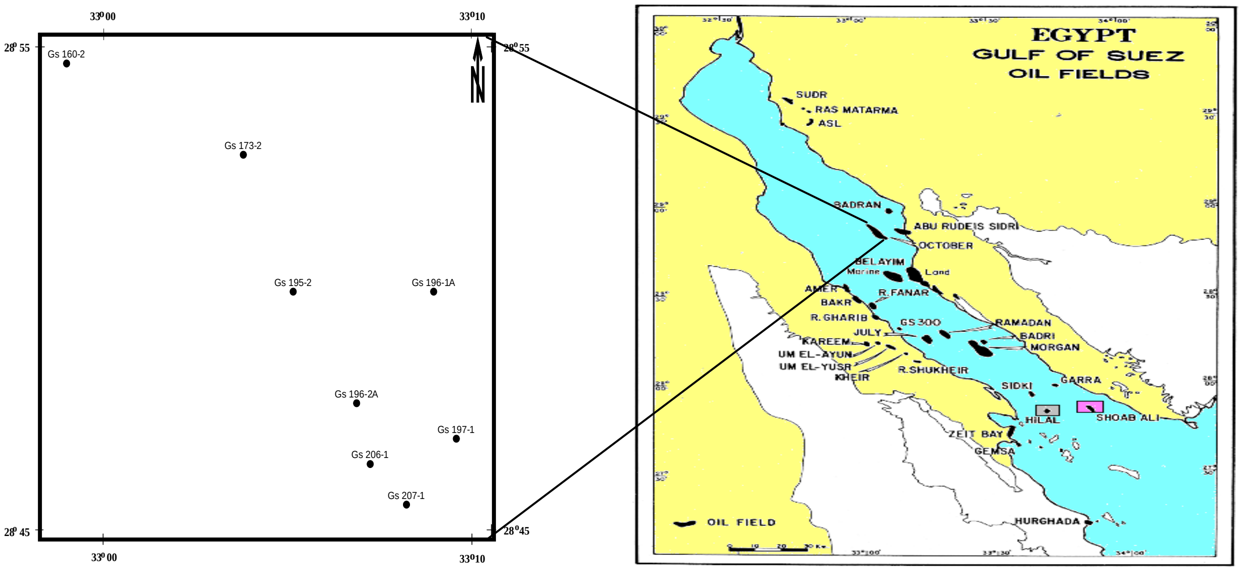

Fig. (1) Location map of the studied wells in October Oil Field, Gulf of Suez, Egypt.

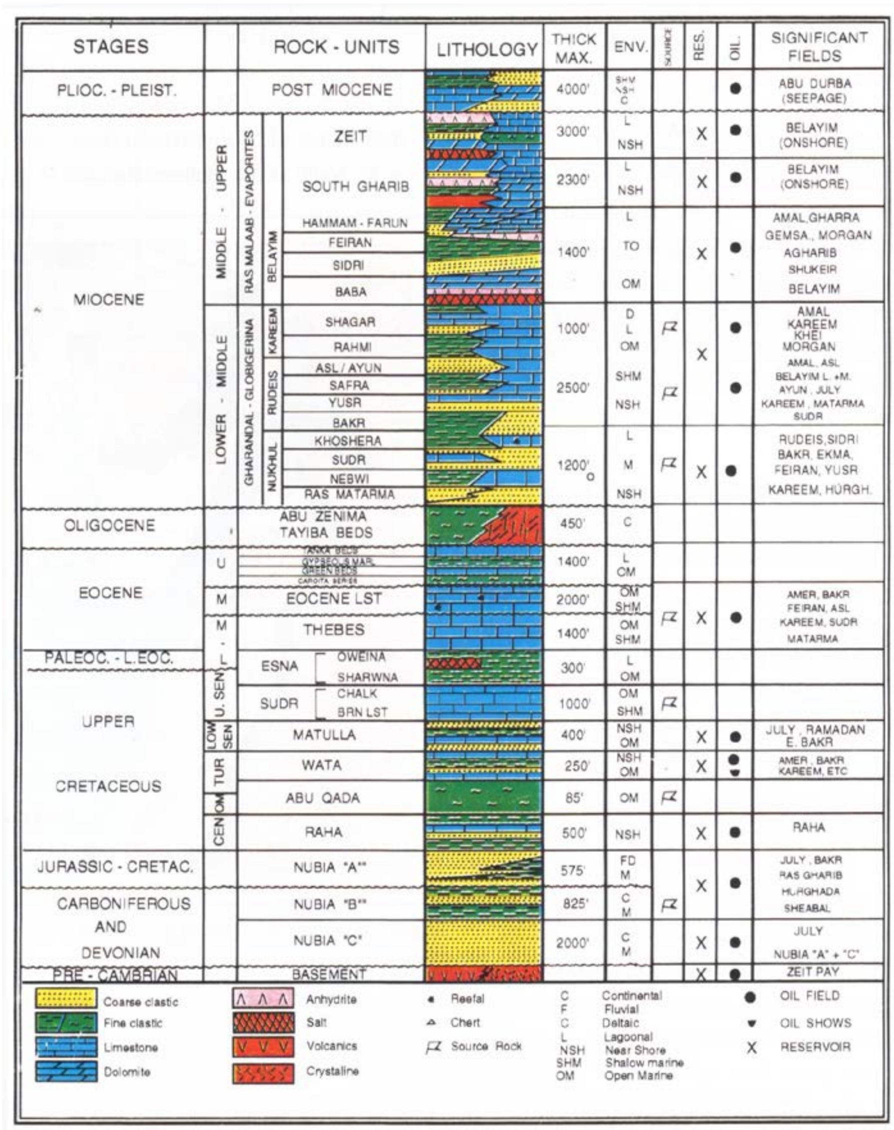

Fig. (2) Generalized litho-stratigraphy of the Gulf of Suez.

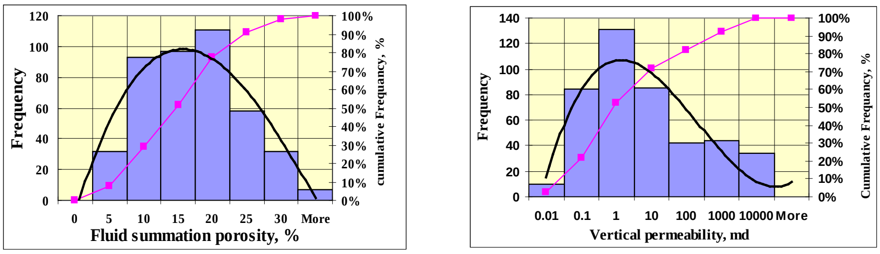

Bin	Frequency	Cumulative %
0	0	.00%
5	32	7.44%
10	93	29.07%
15	97	51.63%
20	111	77.44%
25	58	90.93%
30	32	98.37%
More	7	100.00%

Bin	Frequency	Cumulative %
0.01	10	2.33%
0.1	84	21.86%
1	131	52.33%
10	85	72.09%
100	42	81.86%
1000	44	92.09%
10000	34	100.00%
More	0	100.00%

Fig. (3): Histogram and cummulative frequancy of porosity and permeability of Paleozoic Sediments in October Oil Field, Gulf of Suez, Egypt.

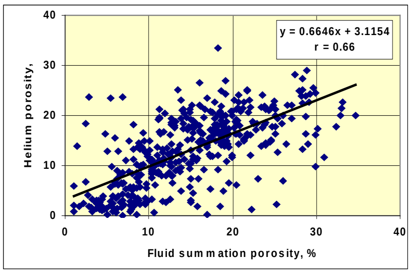

Fig. (4): Relationship between fluid summation porosity and helium Porosity of GS 195-2b well.

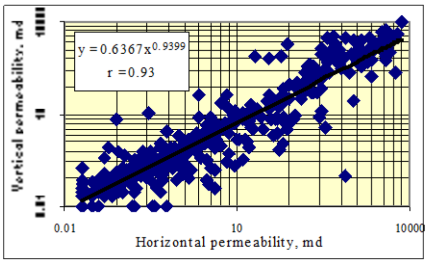

Fig. (5): Relationship between horizontal and vertical permeability of GS 195-2b well.

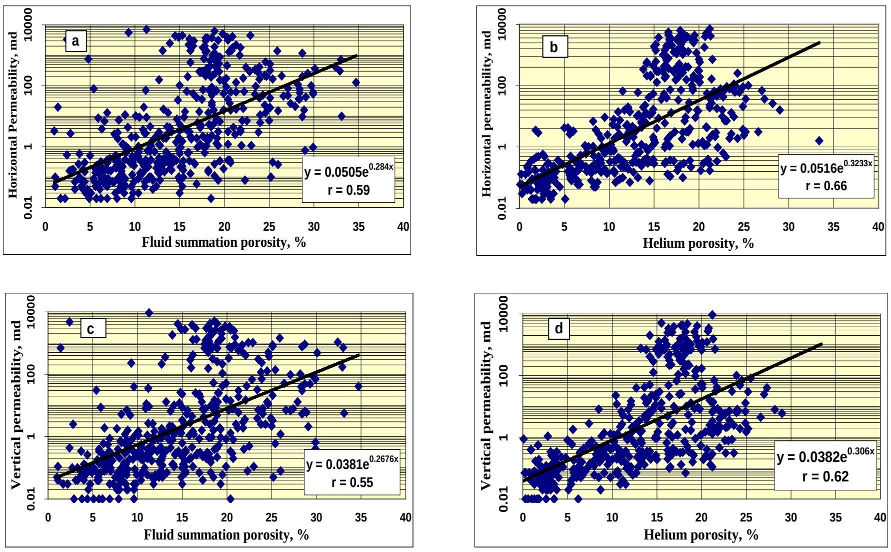

Fig. (6): Porosity-Permeability Relationships of Paleozoic sediments in GS 195-2b well, October Oil Field, Gulf Of Suez, Egypt.

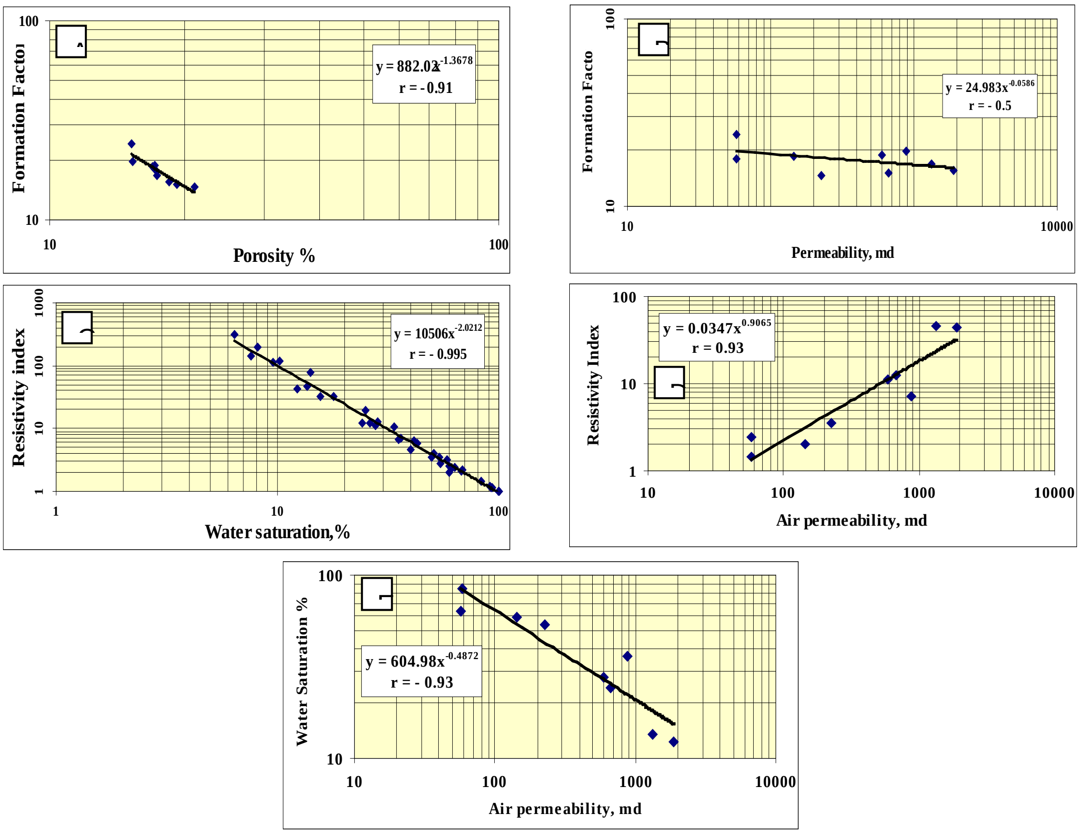

Fig. (7): Relationships between formation factor and porosity, formation factor and permeability, resistivity index and air permeability, water saturation and air permeability and between water saturation and resistivity index of Paleozoic sediments in GS 195-2b, October oil field, Gulf of Suez, Egypt.

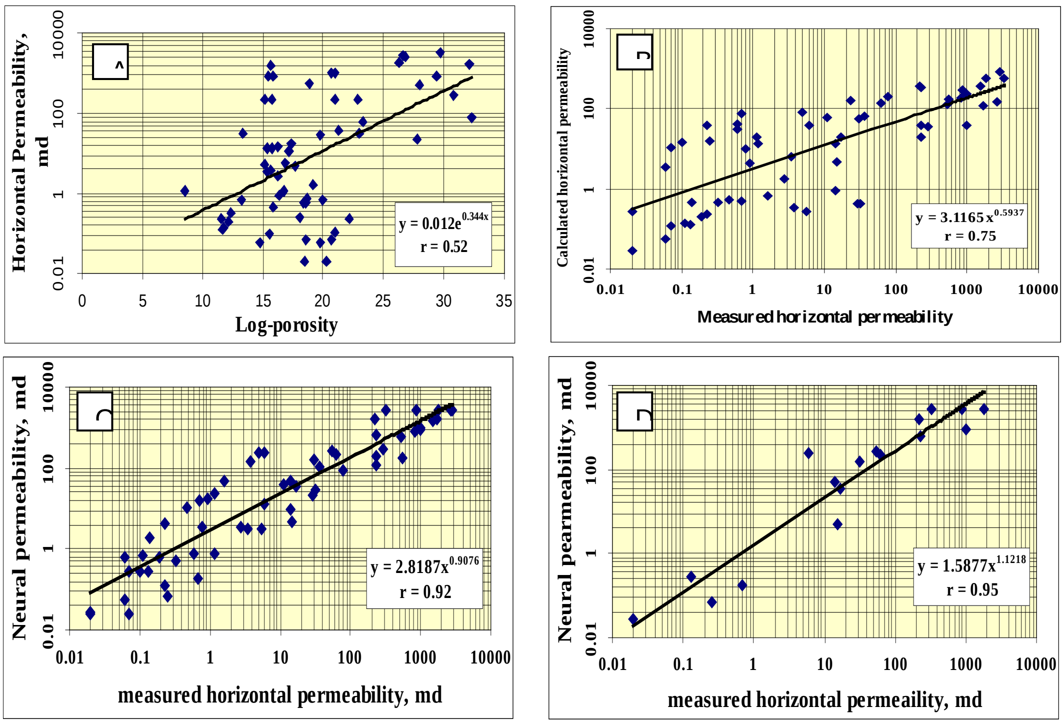

Fig. (8): Permeability estimations by conventional method, optimal transformation method, artificial neural network method for Paleozoic sediments in October Oil Field, Gulf of Suez.

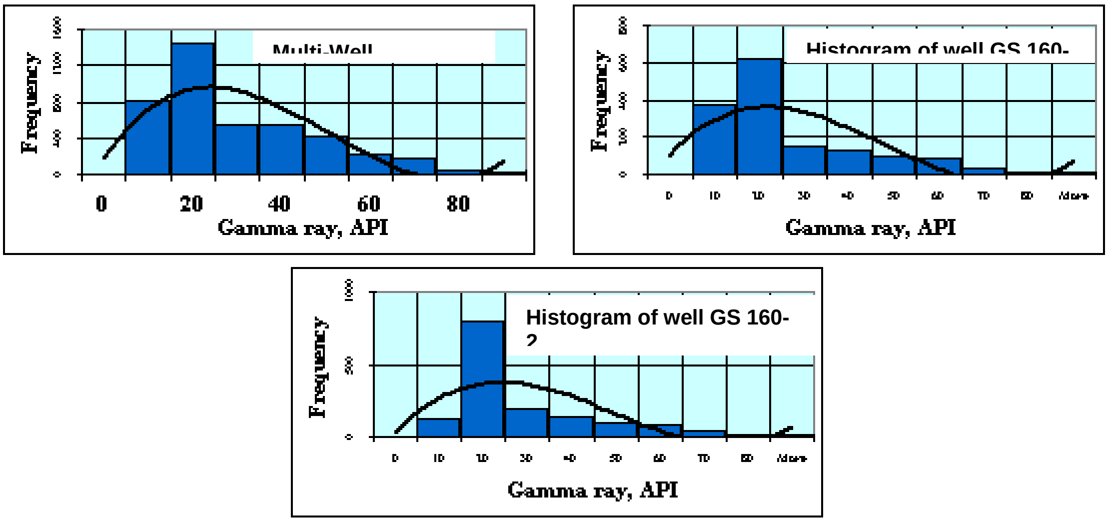

Fig. (9): Normalization histogram of gamma ray log in GS 160-2 well, October Oil Field, Gulf of Suez, Egypt

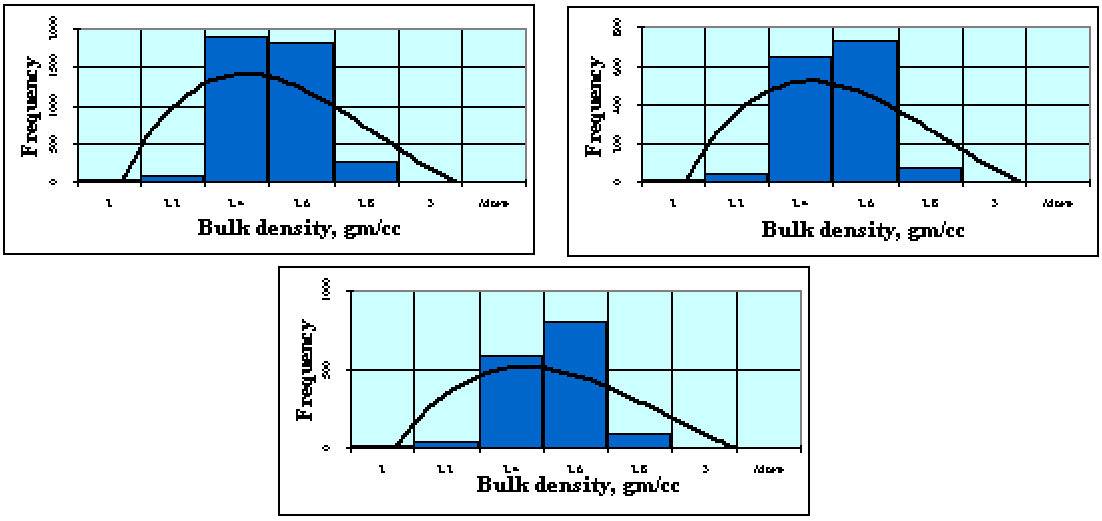

Fig. (10): Normalization histogram of bulk density log in GS 160-2 well, October Oil Field, Gulf of Suez, Egypt

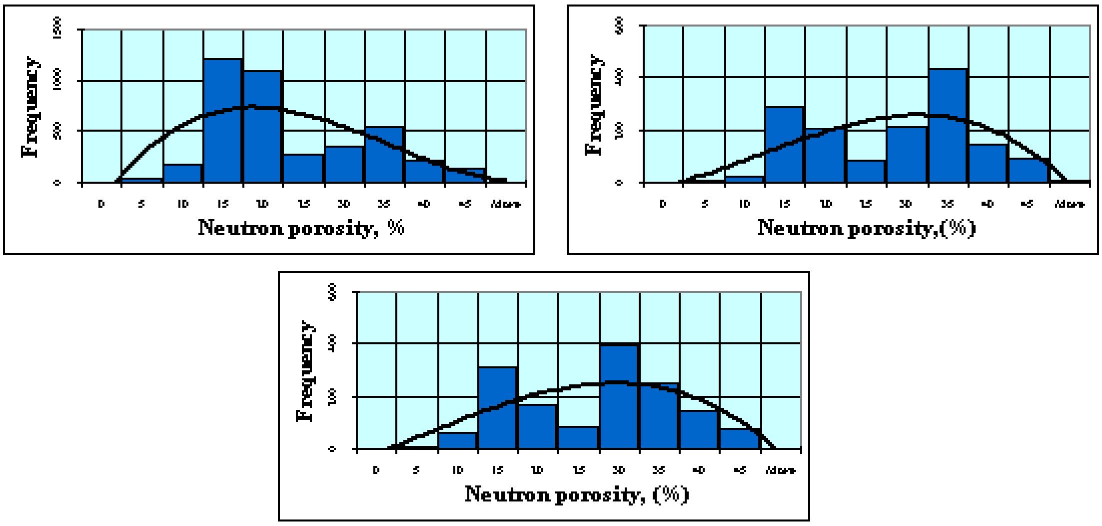

Fig. (11): Normalization histogram of neutron log in GS 160-2 well, October Oil Field, Gulf of Suez, Egypt

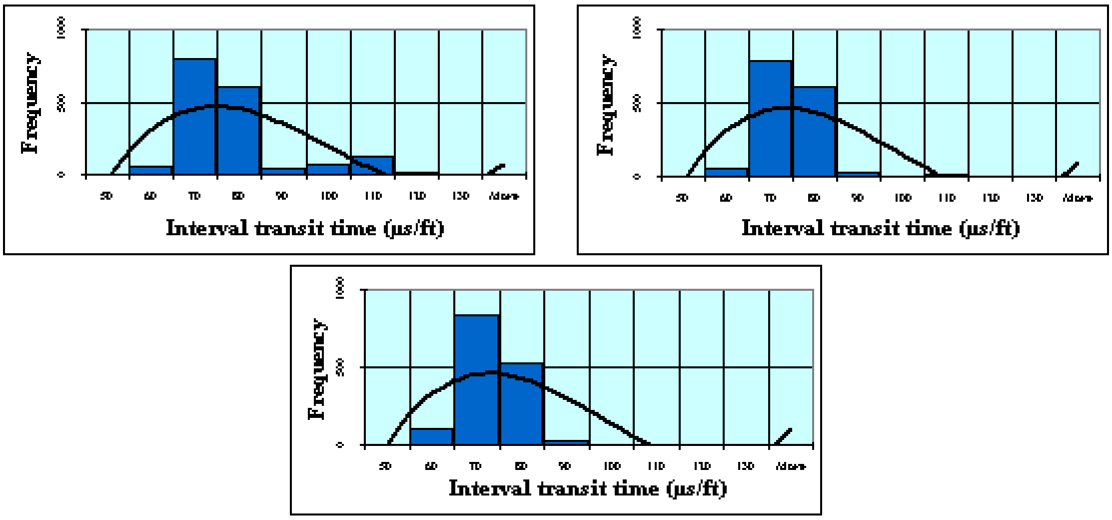

Fig. (12): Normalization histogram of sonic log in GS 160-2 well, October Oil Field, Gulf of Suez, Egypt

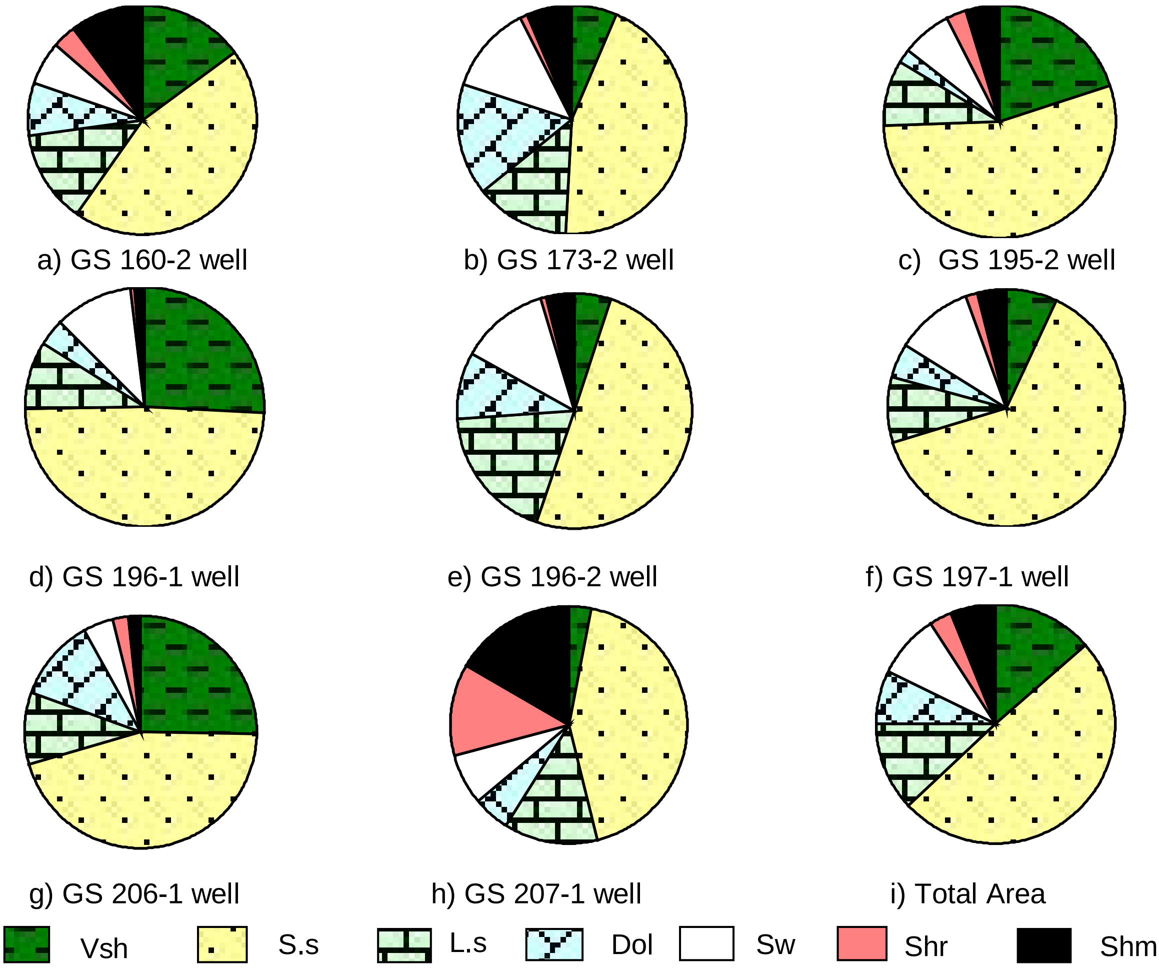

Fig. (13) Total lithosaturation distribution of Paleozoic sediments of the studied wells, October oil field, Gulf of Suez, Egypt.

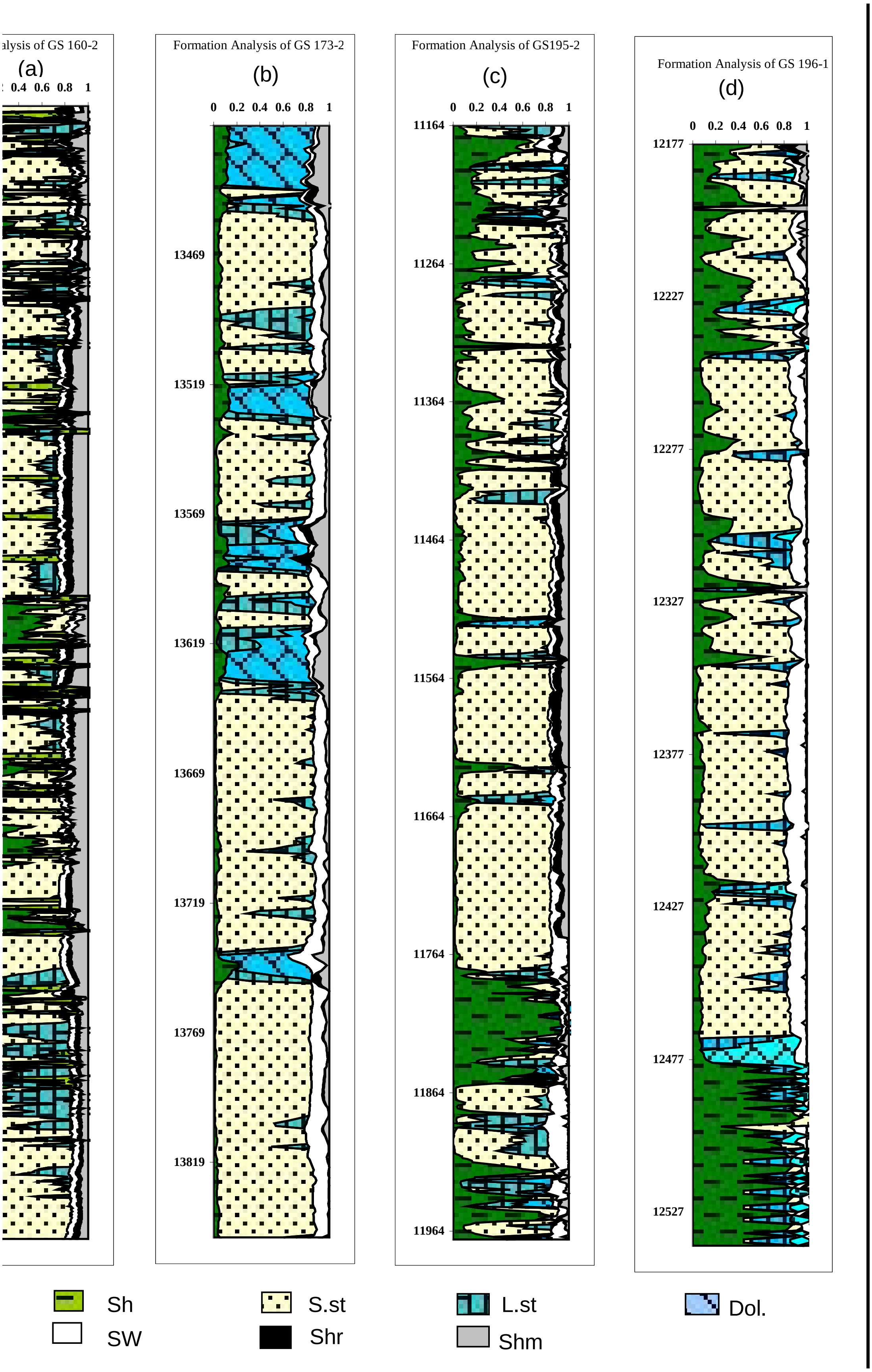

Fig. (14) Formation analysis of Paleozoic sediments in wells GS 160-2, GS 173- 2, GS 195-2 and GS 196-1 October Oil Field, Gulf of Suez, Egypt.

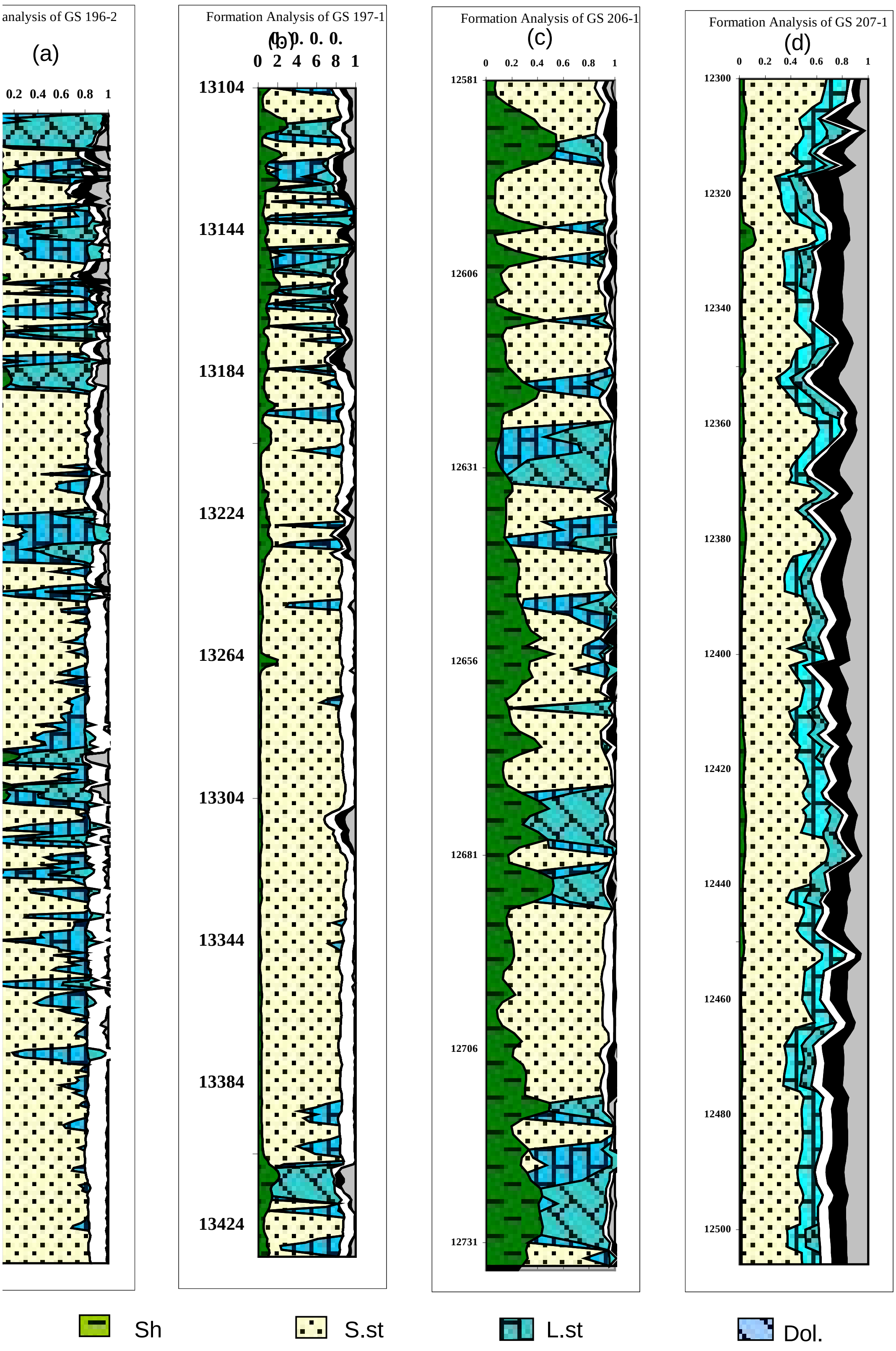

Fig. (15) Formation analysis of Paleozoic sediments in wells GS 196-2, GS 197-1, GS 206-1 and GS 207-1, October Oil Field, Gulf of Suez, Egypt.

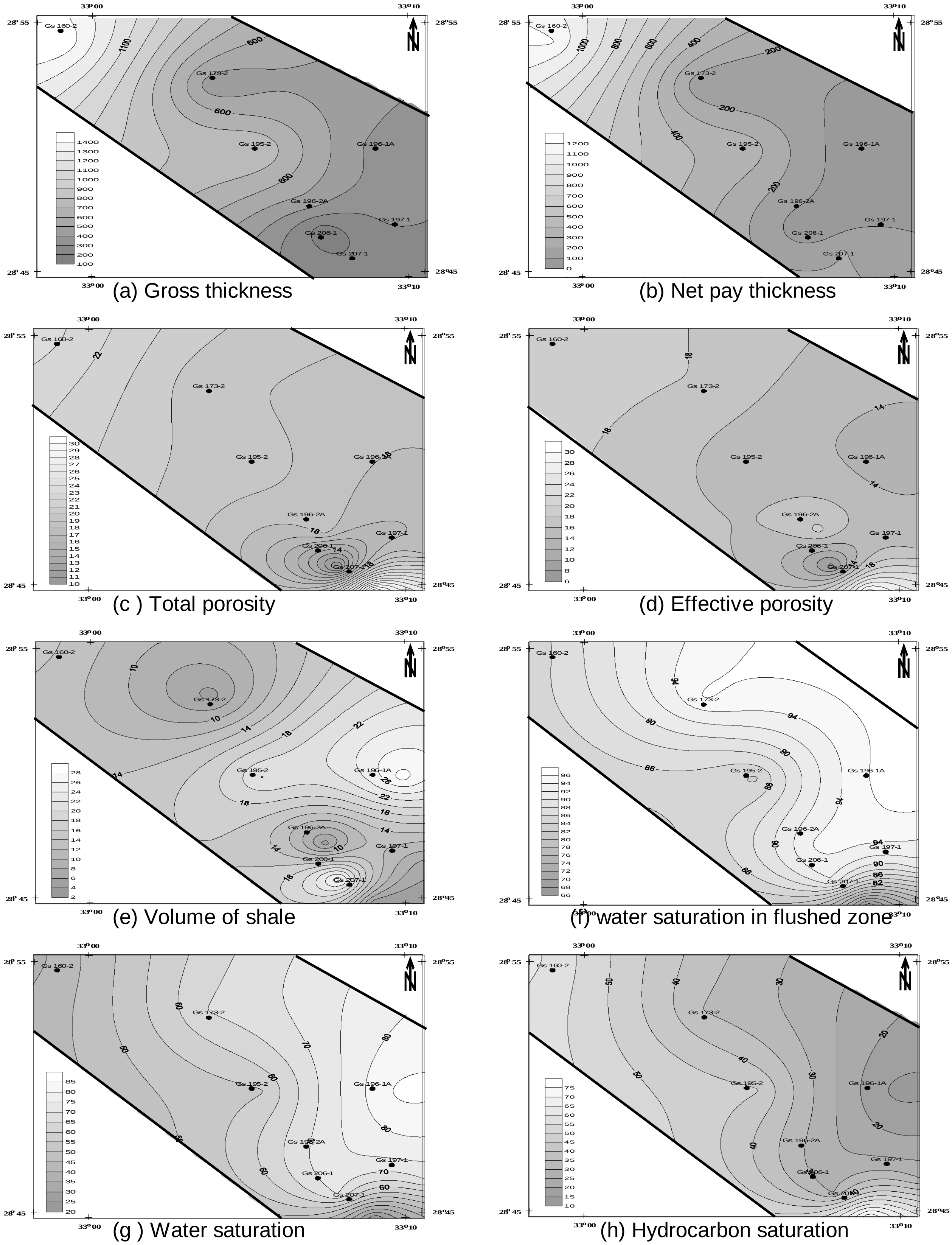

Fig. (16) Formation evaluation parameters of Paleozoic Nubia Formations, October Oil Field, Gulf of Suez, Egypt.

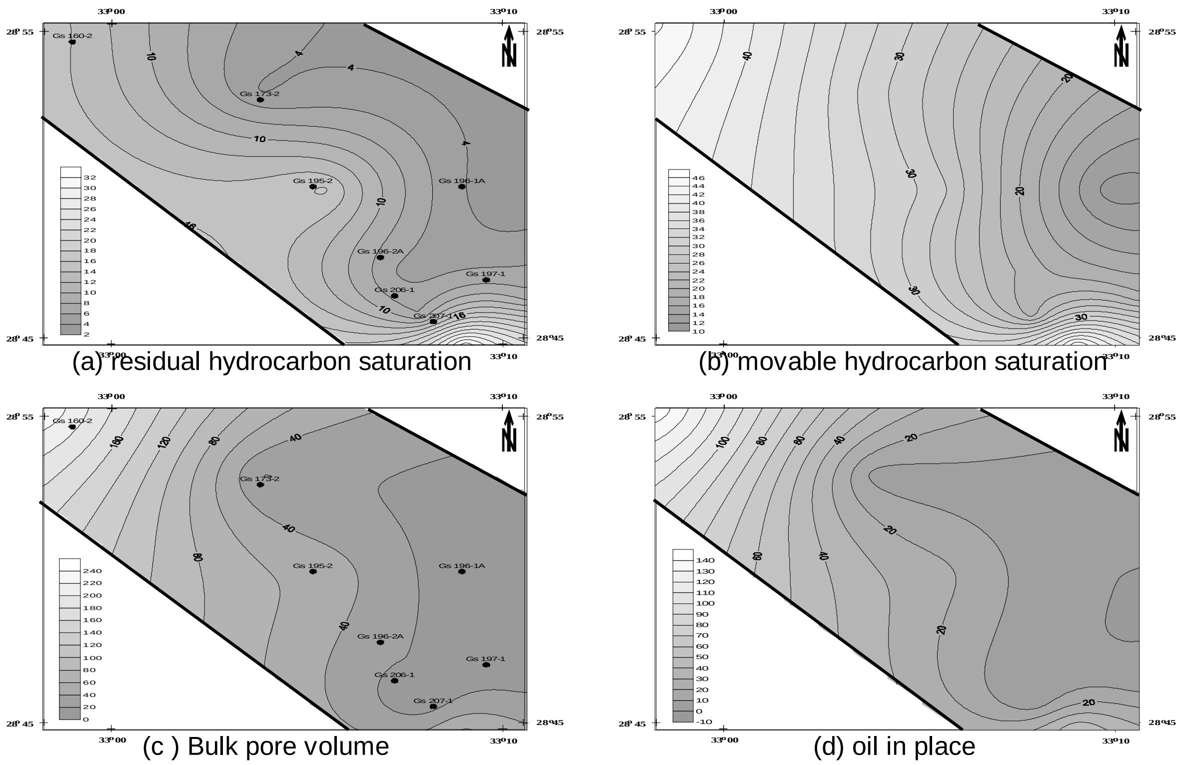

Fig. (17) Formation evaluation parameters of Paleozoic Nubia Formations, October Oil Field, Gulf of Suez, Egypt.

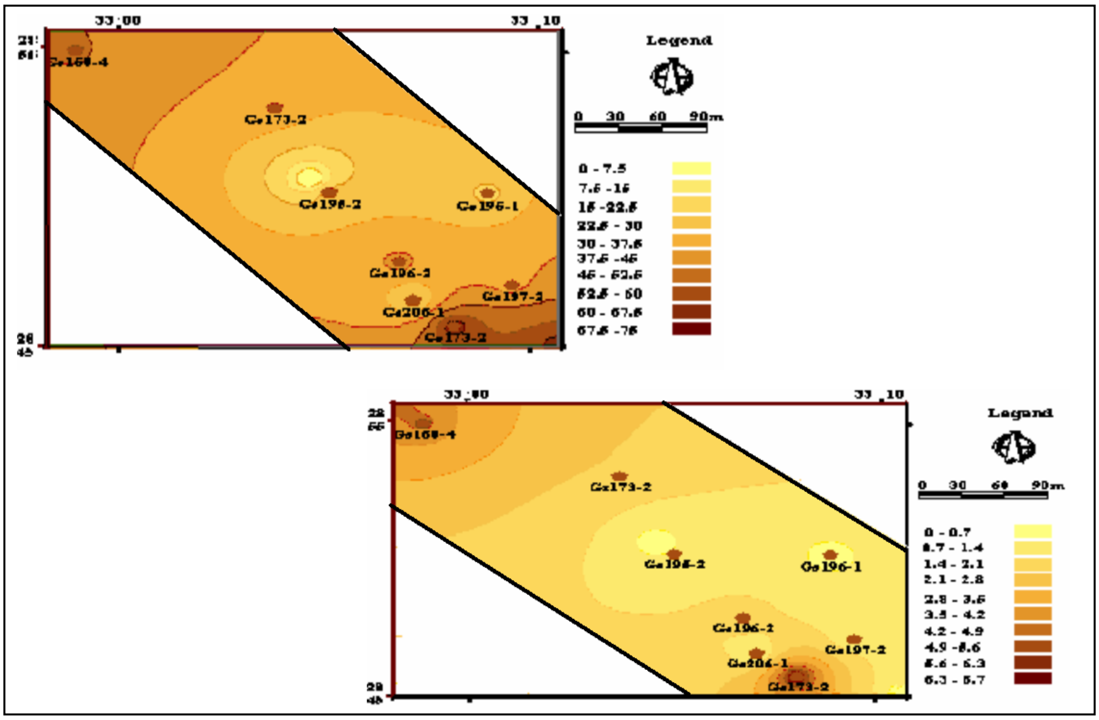

Fig. (18) Development maps for the Paleozoic sediments in October Oil Field, Gulf of Suez, Egypt.

CONCLUSIONS

The study of the petrophysical parameters of the Paleozoic reservoir rocks in October oil field from core and well logging data revealed the following:

1. The reservoir characteristic of Paleozoic sediments in October oil Field reflects the ability of these sediments to store and produce Oil.
2. The results of artificial neural network have clearly demonstrated that, the estimation of permeability from well log data performs significantly better than that of either regression method or optimal transformation.
3. The obtained regression equations of high correlation coefficients are very helpful for calculation of one parameter from the other.
4. Determining the reservoir parameters of Paleozoic sediments such as; total porosity, effective porosity, water saturation, volume of shale, bulk pore volume and oil in place indicator.
5. The Petrophysical maps of Paleozoic sediments parameters reveal that the south and north west directions are the best localities for oil production.

The GIS software was used to estimate the development map which ensure the results of the Petrophysical maps and illustrate this; the south and north west are the best directions to development the October oil Field.

REFERENCES

Breiman, L. and Freidman, J.H., 1985: Estimating optimal transformations for multiple regression and correlation. Jour. Of American Statistical Association, p. 580

Neinast, G.S. and Knox, C.C., 1974: Normalization of well log digitizing, SPWLA 14th Annual Logging Symposium, pp. 18-25.

Thompson, K.A., Franklin, M.H. and Olson, T.M.; 1996: Use of artificial neural nets to predict permeability in Hugoton field, in Abstract. AAPG, Annual Convention official program, Vol. 5, A-135.

Wyllie, M.R.J. and Spangler, M.B.; 1952: Application of electrical resistivity measurements to problem of fluid flow in porous media. Am. Assoc. Petrol. Geol. Bull., p. 359-403